

MEMS based Piezo resistive Pressure Sensor

Swathi Krishnamurthy¹, K.V Meena²,

*E & C Engg. Dept., The Oxford College of Engineering, Karnataka.
 Bangalore 560009*

Abstract

The paper describes the performance analysis and structural design of a silicon piezo resistive pressure sensor using finite element analysis (FEA). The design parameters of the pressure sensor includes membrane shape, the location of piezo resistor and junction depth of piezo resistor. The results depict that proper selection of the membrane geometry and piezo resistor location to enhance the sensor sensitivity.

Keywords-Piezo resistive pressure sensor, finite element analysis (FEA), Parametric analysis.

I INTRODUCTION

Piezo resistance is the name derived from a Greek word “piezin” means “to press”. Change in resistance with respect to stress applied is called as piezo resistive effect. The change in resistance due to applied stress is a function of geometry and resistivity (conductivity) changes. The sensitivity of strain gauge (Gauge Factor) is,

$$GF = \frac{\text{relative change in resistance}}{\text{applied strain}} = \frac{\Delta R / R}{\epsilon} \quad (1a)$$

Piezo resistance is a sensing principle used for MEMS devices. Many MEMS devices such as strain gauges, pressure sensors, force sensors, displacement sensors, chemical sensors utilize the piezo resistive effect.

II THEORY

In general, the electric field E with components E_1 , E_2 , and E_3 in an anisotropic crystal related to the current density j_1 , j_2 and j_3 by the resistivity matrix:

$$\begin{bmatrix} E_1 \\ E_2 \\ E_3 \end{bmatrix} = \begin{bmatrix} \rho_1 & \rho_6 & \rho_5 \\ \rho_6 & \rho_2 & \rho_4 \\ \rho_5 & \rho_4 & \rho_3 \end{bmatrix} \begin{bmatrix} j_1 \\ j_2 \\ j_3 \end{bmatrix}$$

(1b)

For silicon in which the coordinate axes aligns with the $\langle 100 \rangle$ axes, ρ_1, ρ_2, ρ_3 define the resistivity along the $\langle 100 \rangle$ direction and ρ_4, ρ_5, ρ_6 represent the cross resistivities. For unstressed silicon, the resistivity matrix components are

$$\begin{bmatrix} \rho_1 \\ \rho_2 \\ \rho_3 \\ \rho_4 \\ \rho_5 \\ \rho_6 \end{bmatrix} = \begin{bmatrix} \rho \\ \rho \\ \rho \\ 0 \\ 0 \\ 0 \end{bmatrix}$$

(2)

where ρ is the isotropic resistivity. Under a state of stress with tensile components $\sigma_1, \sigma_2, \sigma_3$ and shear components τ_1, τ_2, τ_3 , the fractional change of the resistivity given by

$$\frac{1}{\rho} \begin{bmatrix} \Delta \rho_1 \\ \Delta \rho_2 \\ \Delta \rho_3 \\ \Delta \rho_4 \\ \Delta \rho_5 \\ \Delta \rho_6 \end{bmatrix} = \begin{bmatrix} \pi_{11} & \pi_{12} & \pi_{12} & 0 & 0 & 0 \\ \pi_{12} & \pi_{11} & \pi_{12} & 0 & 0 & 0 \\ \pi_{12} & \pi_{12} & \pi_{11} & 0 & 0 & 0 \\ 0 & 0 & 0 & \pi_{44} & 0 & 0 \\ 0 & 0 & 0 & 0 & \pi_{44} & 0 \\ 0 & 0 & 0 & 0 & 0 & \pi_{44} \end{bmatrix} \begin{bmatrix} \sigma_1 \\ \sigma_2 \\ \sigma_3 \\ \tau_1 \\ \tau_2 \\ \tau_3 \end{bmatrix}$$

(3)

where the piezo-resistivity coefficients $\pi_{11}, \pi_{12}, \pi_{44}$ have units of $1/\text{Pa}$ and can be functions of doping

level and operational temperature .The convention used in the definition of the stresses is illustrated in Figure 1.

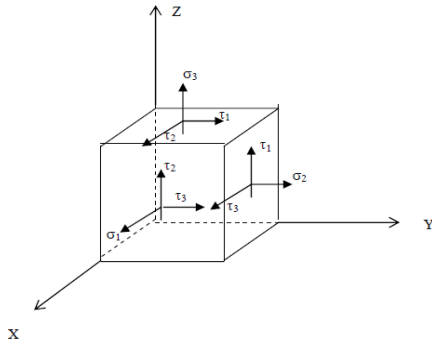


Figure 1: Definition of the stresses

It is often useful to define the fractional change in an arbitrary orientation:

$$\frac{\Delta R}{R} = \sigma_l \pi_l + \sigma_t \pi_t \quad (4)$$

where the subscript l denotes the longitudinal component parallel to the direction of the current and the subscript t denotes transversal components.

II DESIGN CONCEPTS

For the optimum design of sensor sensitivity, the FEA is adopted for the sensor performance design. The design parameters of the pressure sensor include membrane size/shape and piezoresistor location.

MEMS based Pressure sensors are mechanically similar to traditional sensors with the exception that these are Si based and on micrometer scale. The additional advantages of MEMS based pressure sensors include batch fabrication, high performance, small size, low cost, absence of adhesive bonding layer and easy integration with electronics on single chip. Pressure sensors have a wide-range of applications in various fields like automotive industry, biomedical, space applications and military applications. These pressure sensors are available in wide operating range covering from fractions of psi to 15,000 psi.

A lot of research has been carried out on micromachined piezoresistive pressure sensors in the recent years. For high performance demands, the sensitivity and linearity must be improved. In order to increase the sensitivity, the diaphragm thickness should be thin. In

present commercial Piezoresistive pressure sensors, Si diaphragms with less than 20 μm thickness are common . Generally thin diaphragms are prone to large deflections and nonlinear effects. It is therefore necessary to optimize the diaphragm thickness with respect to rigidity and strength.

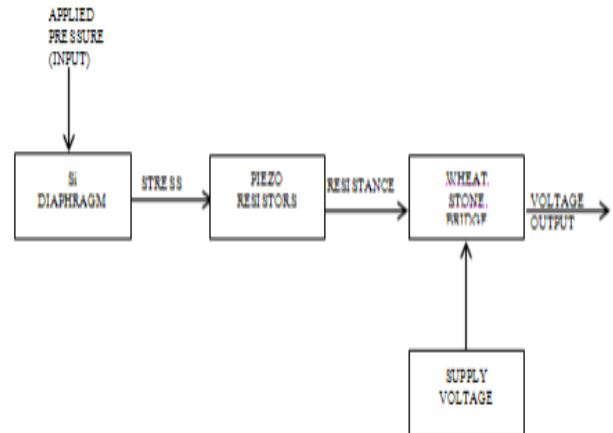


Fig 2: Principle of Piezoresistive pressure sensor.

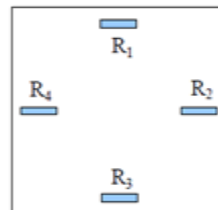


Fig.3 (a): Four piezoresistors on a membrane

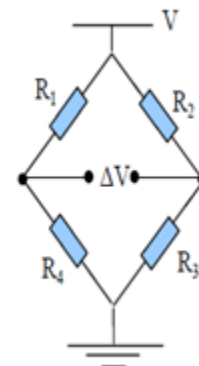


Fig .3(b): Wheatstone bridge configuration of the four piezoresistors

Figure 3 illustrates a membrane with four piezoresistors. Two resistors are oriented to sense stress in the direction of their current axis and two are placed to sense stress perpendicular to their current flow. The

resistors are connected in a Wheatstone bridge (shown in Fig.3), where V is bridge-input voltage, and ΔV is differential output voltage. For the pressure of 0 MPa there will be no change in the resistance, when the stress is applied due to the unbalanced bridge there will be change in the resistance.

The mechanical stresses obtained by FEA should be transferred into output voltage thus the simulation stress value can be applied to predict the equivalent output electrical signal.

This pressure sensing device is composed of four parts: a PCB substrate, a glass substrate bonding with silicon, an adhesive layer between PCB and glass, and a membrane made by silicon with piezoresistive sensing units on it. Figure 4 illustrates the structure cross section of the packaged pressure sensor.

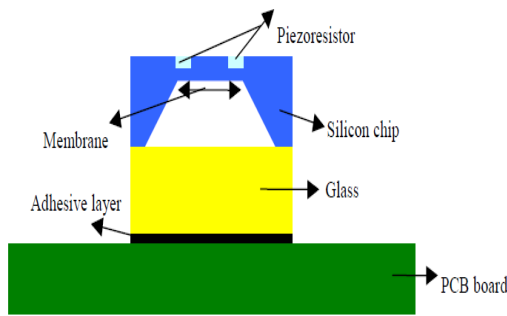


Figure 4: Cross section of the packaged pressure sensor.

The parameters of the study include the location of piezoresistor, the shape of membrane, and the thickness of membrane. The locations of piezoresistor divided into three positions are illustrated in Fig. 5, the three shapes of silicon membrane are shown in Fig.6

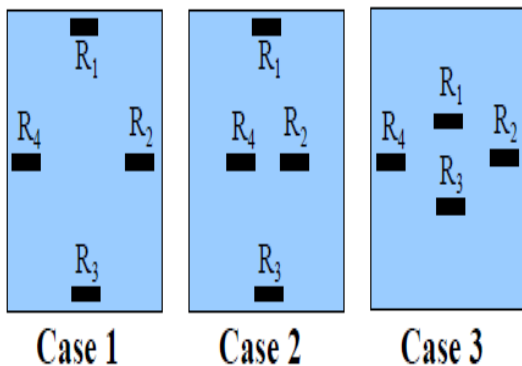


Fig. 5: The three locations of piezoresistors

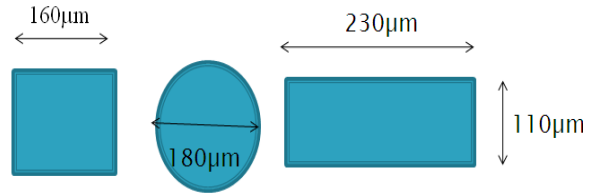


Fig.6: The three shapes of silicon membrane (with the same area but different shape)

Different piezoresistor locations and silicon membrane shapes cause different sensor output voltages, a higher output voltage can enhance the sensor sensitivity and hence increases the sensor application range.

The maximum stress and displacement for rectangle diaphragm are:

$$(\sigma_{yy})_{\max} = \beta \frac{pb^2}{h^2} \tag{5}$$

W = total force acting on the plate, $W = (\pi a)p$ and $m=1/\nu$
 P = applied pressure (MPa), h = thickness of the plate (m)

E = Young's modulus (MPa), and ν = Poisson's ratio

$$w_{\max} = \alpha \frac{pb^4}{Eh^3} \tag{6}$$

in which coefficients α and β can be obtained from Table 1:

a/b	1	1.2	1.4	1.6	1.8	2	∞
α	0.0138	0.0188	0.0226	0.0251	0.0267	0.0277	0.0284
β	0.3078	0.3834	0.4356	0.4680	0.4872	0.4974	0.5000

Table 1: Coefficients for α and β

The maximum stress and displacement for square diaphragm are:

$$\sigma_{\max} = \frac{0.308pa^2}{h^2} \tag{7}$$

$$w_{\max} = -\frac{0.0138pa^4}{Eh^3} \tag{8}$$

The maximum stresses and displacement for circular diaphragm are:

$$(\sigma_{rr})_{\max} = \frac{3W}{4\pi h^2} \tag{9}$$

$$(\sigma_{\theta\theta})_{\max} = \frac{3\nu W}{4\pi h^2} \tag{10}$$

$$W_{\max} = -\frac{3W(m^2 - 1)a^2}{16\pi E m^2 h^3} \tag{11}$$

Figure 6 : Square diaphragm

Table 2: Deflection and stress values for different pressure applied for square diaphragm

III SIMULATION RESULTS

Here the Displacement and stress analysis is carried out with pressure values from 0 to 1MPa in the interval of 0.2Mpa for the square, circle and rectangular diaphragms.

A. For square diaphragm

Sl.No	Pressure Applied (MPa)	Deflection in microns	Stress(Mpa)
1	0.2	0.774951	174.914
2	0.4	1.5499	349.827
3	0.6	2.32485	524.741
4	0.8	3.0998	699.655
5	1	3.87475	874.569

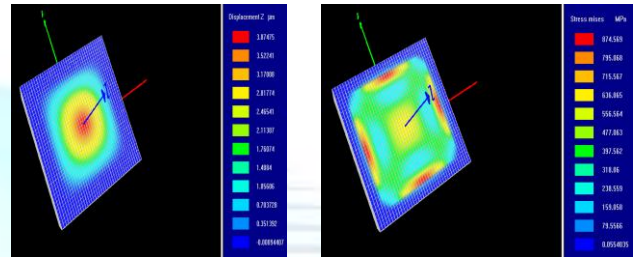


Figure 6 (a): Displacement and stress obtained for 1 MPa

B. For circular diaphragm

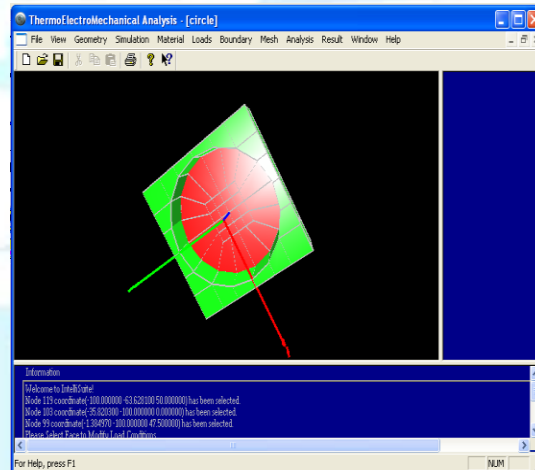


Figure 7: Circular diaphragm

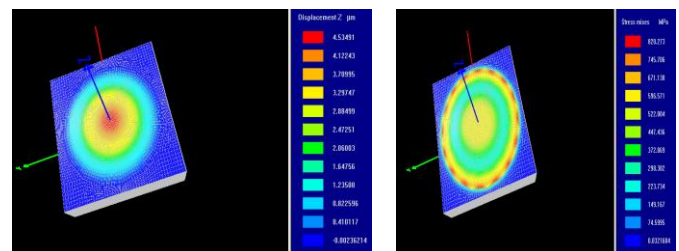
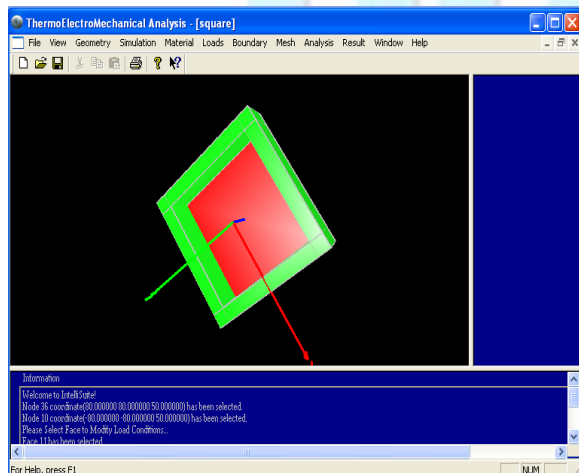


Figure 8 (a): Displacement and stress obtained for 1 MPa

Figure 7 (a): Displacement and stress obtained for 1 MPa

Table 3: Deflection and stress values for different pressure applied for circular diaphragm

Sl.No	Pressure Applied (MPa)	Deflection in microns	Stress (Mpa)
1	0.2	0.906983	164.055
2	0.4	1.81397	328.109
3	0.6	2.72095	492.164
4	0.8	3.62793	656.218
5	1	4.53491	820.273

C. For rectangular diaphragm

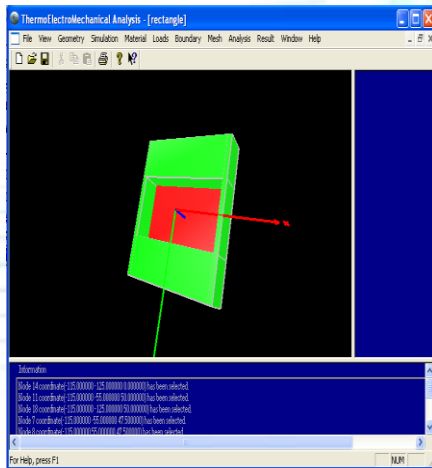
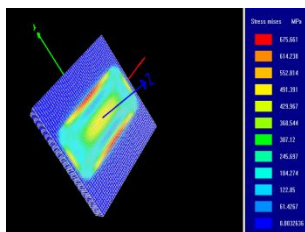
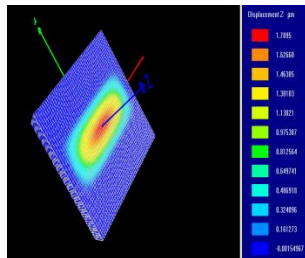


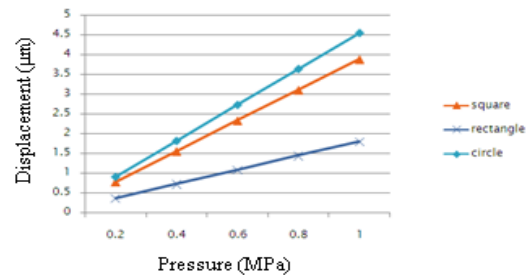
Figure 8: Rectangular diaphragm

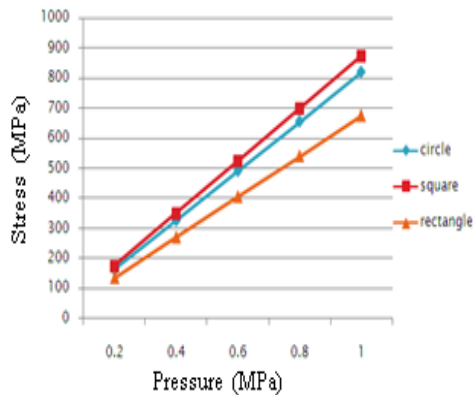
SL.No	Pressure Applied (MPa)	Deflection in microns	Stress(Mpa)
1	0.2	0.3579	135.132
2	0.4	0.7158	270.265
3	0.6	1.0737	405.397
4	0.8	1.4316	540.529
5	1	1.7895	675.661

Table 4: Deflection and stress values for different pressure applied for rectangular diaphragm



COMPARISON





[6] P.J. French and A.G.R. Evans, "Piezoresistance in Polysilicon and Its Applications to Strain Gauges", Solid-State Electronics, Vol.32, No.1, pp.1-10, 1989.

CONCLUSION AND FUTURE WORK

In accordance with the well correlation between experimental and FEA results, the following conclusions are addressed:

According to the results of the parametric studies, it could be found that the circular diaphragm is most favored from design engineering point of view. The square diaphragm has the highest induced stress of all three cases. It is favored geometry for pressure sensors because the high stresses generated by applied pressure loading – result in high sensitivity.

The parametric studies for the different shapes including the piezoresistor at different location should be carried out.

REFERENCES

[1] Tai Ran Hsu, "MEMS and Microsystems Design and Manufacture", Tata Mc-Graw Hill Edition, Tata Mc-Graw Hill, 2002

[2] C.S. Smith, "Piezoresistance Effect in Germanium and Silicon", Physical Review, Vol.94, pp.42-49, 1954.

[3] W.G. Pfann and R.N. Thurston, "Semiconducting Stress Transducers Utilizing the Transverse and Shear Piezoresistance Effects", Journal of Applied Physics, Vol.32, pp.2008 – 2018, 1961.

[4] Y. Kanda, "A Graphical Representation of the Piezoresistance Coefficient in Silicon", IEEE Transactions on Electron Devices, Vol. ED-29, No.1, pp.64-70, 1982.

[5] E. lund and T. Finstad, "Measurement of the Temperature Dependency of the Piezoresistance Coefficients in P-Type Silicon", Advances in Electronic Packaging-ASME, EEP-Vol. 26-1, pp.215-218, 1999.